

A Theoretical Study of the Reaction $\text{H}_2 + \text{Fe}(\text{CO})_4 \rightleftharpoons \text{H}_2\text{Fe}(\text{CO})_4$

Wenhua Wang and Eric Weitz*

Department of Chemistry, Northwestern University, Evanston, Illinois 60208-3113

Received: December 16, 1996[⊗]

Density functional theory (DFT) methods, with three different gradient-corrected functionals (BP86, BLYP, and B3LYP), have been used to calculate molecular geometries and energies along the pathway for oxidative addition of H_2 to $\text{Fe}(\text{CO})_4$ leading to $\text{H}_2\text{Fe}(\text{CO})_4$. The geometry of $\text{H}_2\text{Fe}(\text{CO})_4$, optimized using each of the different functionals, is in good agreement with experimental results. The enthalpies for reductive elimination of H_2 from $\text{H}_2\text{Fe}(\text{CO})_4$, referenced to both the first excited singlet and the triplet ground state of $\text{Fe}(\text{CO})_4$, have been calculated using the BP86, BLYP, and B3LYP functionals and are compared to the experimental result of $21 \pm 2 \text{ kcal mol}^{-1}$. The mechanism for the oxidative addition of H_2 to $\text{Fe}(\text{CO})_4$ is discussed and compared with experimental observations. The geometry of a dihydrogen intermediate, $(\eta^2\text{-H}_2)\text{Fe}(\text{CO})_4$, and the transition state between $(\eta^2\text{-H}_2)\text{Fe}(\text{CO})_4$ and $\text{H}_2\text{Fe}(\text{CO})_4$, along the reaction path, has also been optimized.

I. Introduction

Calculations of the structures and energies of transition metal complexes have proven to be a challenge for conventional Hartree–Fock (HF)-based methods.^{1,2} Extensive treatment of electron correlation is required for the proper description of such systems.^{3–8} In the past few years, density functional theory (DFT)^{9–11} has been shown to be an effective and accurate alternative method for calculations involving transition metal compounds.^{12–17} The inclusion of nonlocal gradient corrections for exchange and correlation has raised the accuracy of DFT calculations to a level that typically can be reached by HF-based methods only with much higher computational cost.^{18,19}

The oxidative addition of H_2 to transition metal centers is an important step in many catalytic processes.²⁰ There have been extensive experimental and theoretical investigations regarding the energetics and mechanism of H_2 oxidative addition to transition metal centers.²¹ The oxidative addition of H_2 to $\text{Fe}(\text{CO})_4$ has recently been studied in the gas phase, by time-resolved IR spectroscopy,²² and the reaction enthalpy for loss of H_2 has been determined.



The possible intermediacy of a dihydrogen species, $(\eta^2\text{-H}_2)\text{Fe}(\text{CO})_4$, along the reaction pathway was mentioned in ref 22 but, to date, has eluded experimental detection.

A theoretical treatment of the reaction of H_2 with $\text{Fe}(\text{CO})_4$ is interesting from several points of view. First, $\text{Fe}(\text{CO})_4$ is one of the best known coordinatively unsaturated organometallic species and has been the subject of extensive experimental and theoretical investigations.²³ Second, the gas-phase molecular structure of $\text{H}_2\text{Fe}(\text{CO})_4$ has been determined by electron diffraction,²⁴ and $\Delta H^{296.5}$ for the reaction has been determined with good accuracy. Both the molecular structure of $\text{H}_2\text{Fe}(\text{CO})_4$ and $\Delta H^{296.5}$ of the reaction can serve as a calibration for theoretical calculations. Third, the simplicity of the ligands and the relatively high symmetry of the system make it convenient to deal with in regard to calculations. Finally, iron carbonyl species are among the most problematic transition metal compounds for conventional *ab initio* calculations.³

In this paper, DFT methods, with gradient corrections for exchange and correlation, are used to study the structures and energies of various species along the pathway for oxidative addition of H_2 to $\text{Fe}(\text{CO})_4$, leading to $\text{H}_2\text{Fe}(\text{CO})_4$. For the purpose of comparison and a test of the methods, the results on the structure and the first CO bond dissociation energy of $\text{Fe}(\text{CO})_5$ are also presented and are discussed first.

II. Computational Methods

Three basis sets were employed, labeled I, II, and III. Basis set I uses Hay and Wadt's effective core potential for Fe which explicitly treats 3s, 3p (the p functions contain some 4p character), 3d, and 4s electrons.²⁵ The use of HF-based effective core potentials in DFT calculations has been shown to give similar results as those for the corresponding all-electron calculations on transition-metal carbonyls.¹⁴ The primitive sets describing 3s, 4s, 3p, and 3d shells are Hay and Wadt's (5/5/5/5), which were contracted to [41/41/2111/41] as suggested in ref 5a. Since the 3s and 4s shells have the same set of exponents, the number of contracted functions is actually [3s/4p/2d]. Basis set I uses 6-31G for C, O, and H.²⁶ Basis set I was used for calculations at HF levels only. Basis set II uses the same effective core potential for Fe as basis set I. The primitive sets for the 3s, 4s, and 3p shells are the same as in basis set I but were contracted to [311/311/2111]. The primitive set for the 3d shell is Wachters' (5d)²⁷ augmented by one set of Hay's diffuse d functions²⁸ and was contracted to [411]. Thus the final number of contracted functions for Fe is [4s/5p/3d]. Basis set II uses 6-31G(p, d) for C, O and H.²⁹ Basis set II was used for most DFT calculations. A larger basis set, basis set III, was used to check the adequacy of basis set II. For Fe, basis set III uses the all electron basis of Wachters' (14s/9p) primitive²⁷ contracted to [5111111111/411111] along with Rappe', Smedley, and Goddard's (6d) contracted to [411].³⁰ Two sets of diffuse p functions²⁷ and one set of f polarization functions (exponent = 2.462)³¹ were added. The final basis set for Fe is [10s/8p/3d/1f]. For C and O, basis set III uses Dunning's (10s/6p)/[5s/3p] triple-zeta basis sets³² supplemented by a set of d polarization functions with exponents of 0.72 and 1.28 for C and O, respectively. For H, basis set III uses Dunning's (5s)/[3s]³² augmented by a set of p polarization functions with an exponent of 1.0. Basis set III was used in some DFT single-point energy calculations at the geometries

[⊗] Abstract published in *Advance ACS Abstracts*, February 15, 1997.

optimized using basis set II. Spherical d and f functions were used throughout.

Three combinations of gradient-corrected functionals for exchange and correlation, BP86, BLYP, and B3LYP, were used in the DFT calculations. BP86 uses Becke's 1988 functional (Slater local functional + Becke's 1988 nonlocal gradient correction) for exchange³³ and Perdew's 1986 functional (Perdew's 1981 local functional + Perdew's 1986 gradient correction) for correlation.³⁴ BLYP uses Becke's 1988 functional for exchange and Lee, Yang, and Parr's functional (which includes both local and gradient corrected terms) for correlation.³⁵ B3LYP uses Becke's three-parameter hybrid functional,³⁶ which has the form

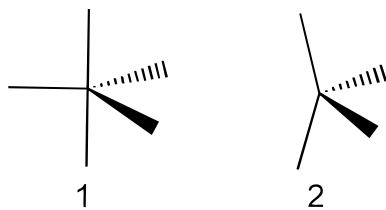
$$E_{XC}^{B3LYP} = AE_X^{Slater} + (1 - A)E_X^{HF} + B\Delta E_X^{Becke} + E_C^{VWN} + C(E_C^{LYP} - E_C^{VWN})$$

where E_X^{Slater} , E_X^{HF} , and ΔE_X^{Becke} are the exchange functionals of Slater, HF, and Becke's 1988 gradient correction term, respectively. E_C^{VWN} is Vosko, Wilk, and Nusair's local functional for correlation,³⁷ and E_C^{LYP} is Lee, Yang, and Parr's functional for correlation. Three parameters, $A = 0.80$, $B = 0.72$, and $C = 0.81$, are taken from those optimized by Becke.³⁶ These three functionals, BP86, BLYP, and B3LYP, have been shown to give good results on metal carbonyls and other transition metal complexes.^{13–17}

All calculations were based on spin-restricted orbitals except those for triplet Fe(CO)₄ where spin-unrestricted orbitals were used.^{38,39} Geometries were optimized using analytical energy first derivatives at the HF⁴⁰ and DFT³⁹ levels, and vibrational frequencies were calculated using analytical energy second derivatives at the HF level.⁴¹ All DFT calculations were done with the "fine grid" option for numerical integration, within the Gaussian 94 package,⁴² on a Cray C-90 supercomputer. HF calculations were carried out with the Gaussian 92 package,⁴³ using an IBM RISC 6000 workstation.

III. Results and Discussion

A. Fe(CO)₅ and Fe(CO)₄. The geometry and the first CO bond dissociation energy of Fe(CO)₅ were calculated as a test of the methods. The geometry of Fe(CO)₅ (**1**) was optimized constrained to D_{3h} symmetry.⁴⁴



The results are shown in Table 1 along with some previous calculations and experimental results. The BP86 and BLYP functionals have previously been shown to give good results for the geometry of Fe(CO)₅. It can be seen from Table 1 that the B3LYP functional also gives good results for the geometry of Fe(CO)₅. The deviation in the bond distances optimized by the DFT methods using the different functionals is less than ~ 0.02 Å. There are some discrepancies in the experimental bond distances for Fe(CO)₅, yet the overall agreement between the calculations and the experimental results is within ~ 0.03 Å. HF-based *ab initio* calculations on the geometry of Fe(CO)₅ give a similar level of accuracy only at the CCI (contracted configuration interactions),³ CASPT2 (complete active space SCF with second-order Moller–Plesset

TABLE 1: Calculated and Experimental Bond Distances (Å) of Fe(CO)₅

	Fe–C _{ax}	Fe–C _{eq}	C–O _{ax}	C–O _{eq}	ref
BP86/II	1.810	1.807	1.162	1.165	this work
BLYP/II	1.832	1.829	1.162	1.166	this work
B3LYP/II	1.829	1.818	1.147	1.151	this work
BP86	1.819	1.816	1.153	1.157	13
BP86	1.806	1.804	1.162	1.165	14
BLYP	1.837	1.834	1.156	1.158	15
MP2	1.688	1.766	1.176	1.666	5b
MP2	1.699	1.791	1.164	1.152	14
MCPF	1.877	1.847	1.168	1.177	4
CCI	1.798	1.835			3
CASPT2	1.792	1.798	1.160	1.160	8
CCSD(T)	1.826	1.826	1.162	1.162	15
expt	1.807	1.827	1.152	1.152	44a
expt	1.811	1.803	1.117	1.133	44b

perturbation),⁸ and CCSD(T) (coupled cluster with single and double excitations and a perturbative treatment of triple excitations) levels.¹⁵ MP2 (second-order Moller–Plesset perturbation) calculations have been reported to give Fe–C distances that are shorter than the experimental values^{5b,14} while MCPF (modified coupled pair functional) calculations have been reported to lead to Fe–C distances that are longer than the experimental values.⁴

The ground state of Fe(CO)₄ adopts a C_{2v} symmetry.^{23,45} The geometry of Fe(CO)₄ (**2**) was optimized within this C_{2v} symmetry constraint. The Fe–C_{ax}–O_{ax} and Fe–C_{eq}–O_{eq} bonds were allowed to bend in the axial and equatorial planes, respectively. The lowest singlet ¹A₁ and lowest triplet ³B₂ states were considered, and the optimized geometries are given in Table 2.

For the lowest singlet state of Fe(CO)₄, the deviation in the bond distances using the different functionals is not significant. The Fe–C_{ax} distance ranges from 1.809 (BP86/II) to 1.825 Å (B3LYP/II), and the Fe–C_{eq} distance ranges from 1.779 (BP86/II) to 1.814 Å (BLYP/II). The BP86/II and B3LYP/II functionals predict that the Fe–C_{ax} distance is 0.02–0.03 Å longer than the Fe–C_{eq} distance, while BLYP/II predicts similar Fe–C_{ax} and Fe–C_{eq} distances. The deviation in the C–O distances is no more than 0.017 Å for all functionals. The BP86/II and B3LYP/II functionals predict that the C_{ax}–Fe–C_{ax} angle is significantly larger than the C_{eq}–Fe–C_{eq} angle. On the other hand, the BLYP/II functional predicts similar C_{ax}–Fe–C_{ax} and C_{eq}–Fe–C_{eq} angles where the equatorial C and O atoms are almost indistinguishable from the axial C and O atoms. The Fe–C–O angles deviate from 180° by $\sim 6^\circ$ – 10° . (The two axial O atoms and two equatorial O atoms bend toward each other in the axial and equatorial planes, respectively.) Since, in prior calculations of the Fe(CO)₄ geometry, the Fe–C–O angles were constrained at 180°, the geometry of Fe(CO)₄ was also optimized with this constraint using BP86/II. The resulting bond distances remain almost identical to those with the Fe–C–O angles unconstrained. The C_{ax}–Fe–C_{ax} and C_{eq}–Fe–C_{eq} angles, however, increase by 11° and 5°, respectively, relative to those calculated with the Fe–C–O angles unconstrained. Thus, the overall conformation of singlet Fe(CO)₄, calculated with the Fe–C–O angles fixed at 180°, is closer to trigonal bipyramidal in which one of the equatorial sites is vacant. The calculated energy for the geometry, optimized with the constraint of Fe–C–O = 180°, is 1.8 kcal mol^{–1} higher than without this constraint.

The geometry of the lowest triplet state of Fe(CO)₄, optimized with the different functionals, shows larger deviations in the Fe–C_{ax} and Fe–C_{eq} distances than those for singlet Fe(CO)₄. The Fe–C_{ax} distance ranges from 1.852 (BP86) to 1.881 Å (B3LYP), and the Fe–C_{eq} distance ranges from 1.816 (BP86)

TABLE 2: Calculated Geometrical Parameters of Singlet and Triplet Fe(CO)₄^a

	Fe–C _{ax}	Fe–C _{eq}	C–O _{ax}	C–O _{eq}	C _{ax} –Fe–C _{ax}	C _{eq} –Fe–C _{eq}	Fe–C _{ax} –O _{ax}	Fe–C _{eq} –O _{eq}	ref
¹ Fe(CO) ₄									
BP86/II	1.809	1.779	1.164	1.169	159.4	132.2	173.6	170.2	this work
BLYP/II	1.813	1.814	1.167	1.167	143.0	142.8	170.1	170.1	this work
B3LYP/II	1.825	1.799	1.150	1.153	154.0	133.9	172.0	169.7	this work
BP86/II	1.813	1.783	1.164	1.169	170.4	137.1	180.0 ^b	180.0 ^b	this work
BP86	1.834	1.793	1.153	1.160	167.7	129.8	180.0 ^b	180.0 ^b	13
MP2	1.726	1.713	1.170	1.178	170.0	135.9	180.0 ^b	180.0 ^b	5b
MCPF	1.910	1.875	1.181	1.178	151	125	180.0 ^b	180.0 ^b	4
³ Fe(CO) ₄									
BP86/II	1.852	1.816	1.163	1.165	150.6	97.8	177.4	179.6	this work
BP86/II	1.851	1.818	1.163	1.165	148.8	97.9	180.0 ^b	180.0 ^b	this work
BLYP/II	1.874	1.844	1.164	1.165	147.8	98.5	178.4	179.7	this work
B3LYP/II	1.881	1.860	1.148	1.150	147.6	98.3	178.5	179.9	this work
BP86	1.859	1.820	1.156	1.160	147.4	99.4	180.0 ^b	180.0 ^b	13
MCPF	1.879	1.885	1.169	1.175	150	104	180.0 ^b	180.0 ^b	4

^a Distances are in angstroms and angles in degrees. ^b Not optimized.

to 1.860 Å (B3LYP). The deviation in the C–O distances is again small, no more than 0.016 Å. The deviation in the angles is small and no more than 3°. The C_{eq}–Fe–C_{eq} angles in the triplet decrease by ~35° in comparison with those of the singlet, and the C_{ax}–Fe–C_{ax} angles are within 9° of those of the singlet. Thus, the structure of triplet Fe(CO)₄ is closer than singlet Fe(CO)₄ to a distorted tetrahedral. On the basis of IR absorption intensities in low-temperature matrices, Poliakoff *et al.* deduced C_{ax}–Fe–C_{ax} and C_{eq}–Fe–C_{eq} angles of 150° and 120° for Fe(CO)₄.^{23,45} The geometry of the triplet state of Fe(CO)₄ was also calculated, using BP86/II, with the Fe–C–O angles constrained to 180°. This calculation gave a geometry and energy that were very similar to those calculated for the triplet state without this constraint. The geometry is indicated in Table 2, and the energy for the constrained geometry was 0.1 kcal/mol higher than the energy for the unconstrained triplet state. This indicates that the optimization of the Fe–C–O angles in the triplet is not as important as in the singlet.

With Fe–C–O angles constrained to 180°, Ziegler and co-workers found similar geometries for singlet and triplet Fe(CO)₄ using gradient-corrected DFT methods with a basis set larger than our basis set II.¹³ Using MCPF methods, Bauschlicher and co-workers⁴ report a geometry for triplet Fe(CO)₄ most similar to that obtained using the B3LYP/II functional in this study. They also reported a partially optimized geometry for singlet Fe(CO)₄. The Fe–C distances are ~0.06–0.1 Å longer than with our DFT results. MP2 calculations by Frenking and co-workers yield a geometry for the singlet state of Fe(CO)₄ with shorter Fe–C distances.^{5b} As mentioned above, MCPF and MP2 calculations have been reported to give Fe–C distances for Fe(CO)₅ that are too long and too short, respectively, when compared to experimental data.

Experimental studies based on magnetic circular dichroism⁴⁶ and kinetics⁴⁷ suggest that Fe(CO)₄ possesses a triplet ground state. Using BP86/II, the triplet is only 0.5 kcal mol⁻¹ below the singlet. The single-point energy calculation using BP86/III with the BP86/II-optimized geometry for both the singlet and triplet states gives the triplet as 0.7 kcal mol⁻¹ below the singlet. Thus, it appears that there is unlikely to be a significant basis set effect on the singlet–triplet energy gap. Ziegler and co-workers found a singlet–triplet separation of 1.7 kcal mol⁻¹.¹³ Using the BP86 functional, but different basis sets and a different algorithm, they optimized the geometries with the constraint of Fe–C–O = 180°. As mentioned above, the optimization of the Fe–C–O angles has a more significant effect on the singlet than on the triplet. Thus, it might be anticipated that if the Fe–C–O angles had been optimized in Ziegler's studies, the resulting singlet–triplet separation would

likely be smaller than 1.7 kcal mol⁻¹. We calculated a singlet–triplet separation of 2.3 kcal/mol using BP86/II with the same Fe–C–O bond angle constraint as Ziegler. The singlet–triplet separation is 0.5 kcal mol⁻¹ using BLYP/II, the same as that for BP86/II. However, it is noted that Delley *et al.* have reported that the triplet is 3 kcal mol⁻¹ above the singlet using the same BLYP functional.¹⁵ The difference between their study and this work is not clear. Using B3LYP/II, the singlet–triplet separation is much larger: with the triplet 8.7 kcal mol⁻¹ below the singlet. The MCPF calculations by Bauschlicher and co-workers⁴ leads to a singlet–triplet separation of 15 ± 5 kcal mol⁻¹, but the MCPF result is likely biased in favor of the triplet.¹⁶

The monocarbonyl species, FeCO, has been the subject of many theoretical calculations.^{19,48} The ground state of FeCO has been shown experimentally to be a ³Σ state with a ⁵Σ state lying 3.7 ± 0.1 kcal mol⁻¹ higher in energy. As part of this study, the quintet–triplet separation of FeCO was calculated to be 5.9, 9.0, and 2.6 kcal mol⁻¹ respectively using BP86/II, BLYP/II, and B3LYP/II. This result is consistent with the result on Fe(CO)₄ in the sense that, in comparison with the BP86 and BLYP functionals, the B3LYP functional favors higher spin multiplicity states.

There is no experimental value for the singlet–triplet separation in Fe(CO)₄. Time-resolved IR studies show that 351 nm photolysis of gas-phase Fe(CO)₅ produces two distinct Fe(CO)₄ species: a ground-state triplet Fe(CO)₄ and an electronically excited Fe(CO)₄*.⁵⁰ Fe(CO)₄* can relax to triplet Fe(CO)₄ by collisions. It was reported that Fe(CO)₄* is likely to be the lowest singlet state of Fe(CO)₄, which can be generated by the photodissociation of Fe(CO)₅ on its lowest singlet potential energy surface. However, after complete relaxation of photo-products, no detectable Fe(CO)₄* was observed. If the singlet and triplet states of Fe(CO)₄ are in equilibrium, on the time scale of this experiment, a singlet–triplet separation of 1.5 kcal mol⁻¹ will lead to an appreciable amount of Fe(CO)₄* (~8%) in equilibrium with ground-state Fe(CO)₄. Thus, if such an equilibrium exists, the singlet–triplet separation is likely to be larger than 1.5 kcal mol⁻¹.

Table 3 shows the calculated first CO bond dissociation energy, ΔE, and enthalpy, ΔH²⁹⁸, of Fe(CO)₅. The thermal correction was taken from ref 56 in converting ΔE to ΔH²⁹⁸. This can be compared to a recent experimental value of 42 ± 2 kcal mol⁻¹.⁵¹ This value was assigned to the first CO bond dissociation enthalpy of Fe(CO)₅ relative to singlet Fe(CO)₄ + CO. As can be seen from Table 3, the result for BP86/II is larger than the experimental result while those using BLYP/II and B3LYP/II are smaller. However, for each case, the

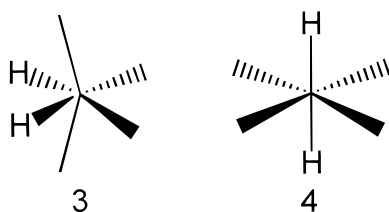
TABLE 3: Calculated and Experimental First CO Bond Dissociation Energies (kcal/mol) of Fe(CO)₅^a

	ΔE		ΔH^{298}		ref
	singlet	triplet	singlet	triplet	
BP86/II	45.9	45.4	45.4	44.9	this work
BLYP/II	38.4	37.9	38.0	37.5	this work
B3LYP/II	38.7	30.0	38.4	29.7	this work
BP86	44.8	43.0			13
BLYP	38	41			15
MCPF	39 ± 5	23.9			4
CCSD(T)//MP2	46.9		46.5		5b
expt			42 ± 2		49

^a The values in the singlet and triplet columns are relative to the lowest singlet and triplet states of Fe(CO)₄, respectively.

agreement between the calculations and the experiment is within 5 kcal mol⁻¹. Thus, each of the three functionals gives good results regarding the geometry and the enthalpy for loss of the first CO from Fe(CO)₅.

B. H₂Fe(CO)₄. The possibility of cis (**3**) and trans (**4**) isomers of the dihydride species, H₂Fe(CO)₄, has been considered in previous investigations.



Electron diffraction²⁴ and spectroscopic studies⁵² indicate that H₂Fe(CO)₄ adopts a cis geometry in its ground state. However, at HF levels, it has been reported that the trans isomer is more stable than the cis isomer for H₂Fe(CO)₄ and related compounds.⁵³ A recent CASSCF study concluded that the inclusion of nondynamical s and p correlation effects is necessary to account for the ordering of the experimentally determined energies and the Fe–C bond distances of the two isomers.⁵⁴

The geometry of *cis*-H₂Fe(CO)₄ was optimized within the constraint of C_{2v} symmetry using the aforementioned three functionals. The geometry of *trans*-H₂Fe(CO)₄ was optimized within the constraint of D_{4h} symmetry using the BP86 functional. Using BP86/II, the cis isomer is more stable than the trans isomer by 11.3 kcal mol⁻¹. Thus, DFT with gradient correction predicts the correct energy ordering of the isomers of H₂Fe(CO)₄. All DFT calculations predict similar geometries for the cis isomer of H₂Fe(CO)₄, which are in good agreement with the electron diffraction results (see Table 4). The biggest error in bond distances is for the H–H distance: the calculated results are more than 0.3 Å too short relative to experimental results.²⁴ All other bond distances, including the Fe–C and Fe–H distances, are within 0.04 Å of the experimental results. The DFT results indicate that the Fe–C_{ax} distance is shorter than the Fe–C_{eq} distance by about 0.02 Å. On the other hand, the electron diffraction study shows that the Fe–C_{ax} distance is about 0.03 Å longer than the Fe–C_{eq} distance. The calculated C_{ax}–Fe–C_{ax} and C_{eq}–Fe–C_{eq} angles are ~4° too large. The calculated Fe–C_{ax}–O_{ax} angles are almost reproduced by these calculations. The calculated Fe–C_{eq}–O_{eq} angles are ~12° too small. However, the calculations predict correctly that the Fe–C_{eq}–O_{eq} angle is larger than 180°, i.e., the two equatorial O atoms move further away from each other in the equatorial plane.

The calculated reaction energy and enthalpy for the reductive elimination of H₂ from H₂Fe(CO)₄ are shown in Table 5. In

converting the reaction energy, ΔE , to the reaction enthalpy, $\Delta H^{296.5}$, vibrational frequencies calculated at the HF/I level were used. The effect of zero-point energy, vibrational excitation, translation, rotation, and work term (ΔPV) corrections leads to a value of $\Delta H^{296.5}$ 2.3 kcal mol⁻¹ smaller than ΔE . The experimental value for $\Delta H^{296.5}$ is 21 ± 2 kcal mol⁻¹.²² As noted in ref 22, the experimental value is most likely relative to the triplet Fe(CO)₄. Using BP86/II, $\Delta H^{296.5}$ relative to the triplet Fe(CO)₄ is 23.4 kcal mol⁻¹. A single-point calculation using BP86/III with the geometry optimized with BP86/II leads to a value of 24.7 kcal mol⁻¹ for $\Delta H^{296.5}$. Since the calculated value using the two different basis sets differs by only 1.3 kcal mol⁻¹, this again indicates the adequacy of basis set II. Calculations with B3LYP/II give a value of 12.9 kcal mol⁻¹ for $\Delta H^{296.5}$ relative to the triplet Fe(CO)₄, significantly smaller than the experimental value. The calculation with BLYP/II for $\Delta H^{296.5}$ is even smaller; only 11.1 kcal mol⁻¹. As discussed in ref 22, though conventional wisdom indicates that dissociation of H₂Fe(CO)₄ should be referenced to the triplet ground state of Fe(CO)₄, the existing experimental data on this system do not allow one to unambiguously determine whether the dissociation of H₂Fe(CO)₄ should be referenced to the triplet ground state of Fe(CO)₄ or to the somewhat higher energy singlet state. If dissociation should be referenced to the singlet state, then the B3LYP functional gives the best agreement with experimental data. If the reference for dissociation of H₂Fe(CO)₄ should be the triplet state, then the agreement between experimental results and calculations using B3LYP is not nearly as good due to the relatively large singlet–triplet separation calculated using this functional. However, the BP86 functional gives good results independent of whether the dissociation process should be referenced to the first excited singlet or the triplet ground state of Fe(CO)₄. This occurs since the singlet–triplet separation in Fe(CO)₄, calculated using the BP86 functional, is small relative to the H₂Fe(CO)₄ bond dissociation enthalpy. In either case the BLYP functional does not give good agreement with experimental data. It should be noted that prior calculations on main group compounds⁵⁵ and transition metal monocarbonyls^{48a} have shown that the B3LYP functional often gives results that are superior to other functionals.

C. (η^2 -H₂)Fe(CO)₄ and the Transition State. The oxidative addition of H₂ to metal centers is commonly accepted to occur via a concerted mechanism with a dihydrogen species as a potential intermediate.⁵⁶ Thus, a dihydrogen species, (η^2 -H₂)Fe(CO)₄, was first located at the HF/I level. The (η^2 -H₂)Fe(CO)₄ species, optimized at the HF/I level, constrained to C_{2v} symmetry, has a H–H distance of 0.837 Å and a Fe–H distance of 1.678 Å. That this species represents a local minimum on the potential energy surface was confirmed by a calculation of vibrational frequencies. A transition state (TS) between (η^2 -H₂)Fe(CO)₄ and H₂Fe(CO)₄ was also located at the HF/I level, again within C_{2v} symmetry constraints. It has an H–H distance of 0.943 Å and an Fe–H distance of 1.622 Å. The vibrational frequency calculation shows one imaginary frequency. The vibration associated with this imaginary frequency is largely dominated by stretching of the H–H bond but also contains small contributions from the translation of the H₂ molecule toward the Fe(CO)₄ fragment. The geometries of (η^2 -H₂)Fe(CO)₄ and the TS were reoptimized in calculations using BP86/II and are shown in Table 4. The H–H distance is now 0.924 Å in (η^2 -H₂)Fe(CO)₄ and 1.109 Å in the TS, compared to 2.006 Å in H₂Fe(CO)₄. The Fe–H distance decreases from 1.604 Å in (η^2 -H₂)Fe(CO)₄ to 1.544 Å in the TS and 1.525 Å in H₂Fe(CO)₄. Thus, the H–H distance in the TS is close to that in (η^2 -H₂)Fe(CO)₄ while the Fe–H distance in the TS is similar

TABLE 4: Geometrical Parameters of $\text{H}_2/\text{Fe}(\text{CO})_4$ Species^a

	Fe–H	H–H	Fe–C _{ax}	Fe–C _{eq}	C–O _{ax}	C–O _{eq}	C _{ax} –Fe–C _{ax}	C _{eq} –Fe–C _{eq}	Fe–C _{ax} –O _{ax}	Fe–C _{eq} –O _{eq}
<i>cis</i> - $\text{H}_2\text{Fe}(\text{CO})_4$										
BP86/II	1.525	2.006	1.794	1.809	1.161	1.161	152.0	99.8	175.3	182.0
BLYP/II	1.532	2.017	1.815	1.834	1.161	1.161	152.9	99.9	175.1	182.2
B3LYP/II	1.519	2.020	1.808	1.827	1.146	1.146	152.8	100.5	174.8	182.5
expt ^b	1.556	2.384	1.832	1.802	1.145	1.145	148.5	96.0	176.2	194.5
<i>trans</i> - $\text{H}_2\text{Fe}(\text{CO})_4$										
BP86/II	1.533			1.801		1.160				
$(\eta^2\text{-H}_2)\text{Fe}(\text{CO})_4$										
BP86/II	1.604	0.924	1.810	1.794	1.162	1.166	177.6	118.6	179.9	178.8
TS										
BP86/II	1.544	1.109	1.806	1.802	1.161	1.164	172.0	112.9	178.8	180.9

^a Distances are in Å and angles in deg. ^b Reference 24.

TABLE 5: Calculated and Experimental Reaction Enthalpy (kcal/mol) for the Reductive Elimination of H_2 from $\text{H}_2\text{Fe}(\text{CO})_4$ ^a

	$-\Delta E$		$-\Delta H$	
	singlet	triplet	singlet	triplet
BP86/II	26.2	25.7	23.9	23.4
BLYP/II	13.9	13.4	11.6	11.1
B3LYP/II	23.9	15.2	21.6	12.9
expt ^b				21 ± 2

^a The values in the singlet and triplet columns are relative to the lowest single and triplet states of $\text{Fe}(\text{CO})_4$ respectively. ^b Reference 22.

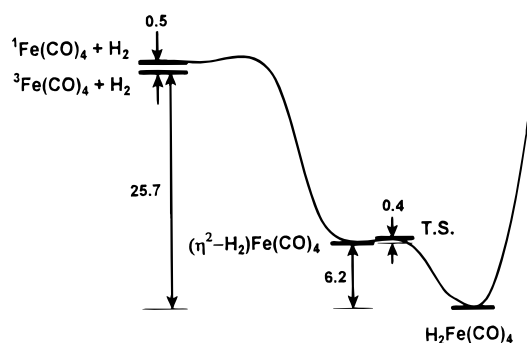


Figure 1. A diagram of the change in energy (kcal/mol) for the $\text{H}_2 + \text{Fe}(\text{CO})_4$ system along the reaction coordinate based on BP86/II calculations.

to that in $\text{H}_2\text{Fe}(\text{CO})_4$. That is, in the TS, in going from the dihydrogen to the dihydride species, there is significant formation of the Fe–H bonds *before there is substantial elongation and breaking of the H–H bond*. This is consistent with a low activation barrier for the transformation and calculations using BP86/II indicate that the TS is only 0.4 kcal mol⁻¹ above $(\eta^2\text{-H}_2)\text{Fe}(\text{CO})_4$. The dihydrogen species $(\eta^2\text{-H}_2)\text{Fe}(\text{CO})_4$ was calculated to be 6.2 kcal mol⁻¹ above the dihydride species, $\text{H}_2\text{Fe}(\text{CO})_4$, using BP86/II.

Figure 1 shows a diagram of the potential energy surface for the $\text{H}_2\text{-Fe}(\text{CO})_4$ along the reaction coordinate. The relative energies of the stationary points are those calculated using BP86/II. Only one point, $^3\text{Fe}(\text{CO})_4 + \text{H}_2$, was calculated on the triplet surface. The activation barrier on the singlet surface for the formation of $(\eta^2\text{-H}_2)\text{Fe}(\text{CO})_4$ from $^1\text{Fe}(\text{CO})_4 + \text{H}_2$ was not determined in this study but is expected to be low. Ziegler *et al.* have estimated an activation barrier of 3–11 kJ mol⁻¹ for the addition of H_2 to singlet $\text{M}(\text{CO})_4$ ($\text{M} = \text{Ru}$ and Os).⁵⁷ They also found dihydrogen complexes, $(\eta^2\text{-H}_2)\text{M}(\text{CO})_4$, which are located in a flat local minima along the reaction course and have H–H distances of 1.04–1.12 Å. Since the reactants are $^3\text{Fe}(\text{CO})_4 + \text{H}_2$, and the product, $\text{H}_2\text{Fe}(\text{CO})_4$, is expected to be a singlet, a crossing from triplet to singlet potential energy surfaces occurs at the same point along the reaction path. The

energy of the crossing point, relative to $^3\text{Fe}(\text{CO})_4 + \text{H}_2$, cannot exceed the singlet–triplet separation plus the activation barrier on the singlet surface. Even if the singlet–triplet spacing is not as small as the calculated value of 0.5 kcal mol⁻¹, it is still expected to be on that order, and since the singlet surface has a low activation barrier, the energy of the crossing point relative to $^3\text{Fe}(\text{CO})_4 + \text{H}_2$ is not expected to be high. That is, the activation barrier for the oxidative addition of H_2 to triplet $\text{Fe}(\text{CO})_4$ should not be high. Experimentally, the upper bound for this barrier has been estimated to be 4 kcal mol⁻¹.²² After the curve crossing, the reaction will proceed on the singlet surface. Since $(\eta^2\text{-H}_2)\text{Fe}(\text{CO})_4$ represents a very shallow local minimum, it is likely that, in the gas phase, at the room temperature, the reaction will pass through this local minimum directly to the $\text{H}_2\text{Fe}(\text{CO})_4$ product. Thus, it is not surprising that no intermediate has been observed in the experiments performed to date.²²

IV. Conclusions

DFT with gradient corrections for exchange and correlation is used to study the structures and the bond dissociation energies of $\text{Fe}(\text{CO})_5$ and $\text{H}_2\text{Fe}(\text{CO})_4$. All three functionals, BP86, BLYP, and B3LYP, yield geometries for $\text{Fe}(\text{CO})_5$ and $\text{H}_2\text{Fe}(\text{CO})_4$ that are in good agreement with experimental results. The first CO bond dissociation enthalpy for $\text{Fe}(\text{CO})_5$, calculated using the three functionals, is in good agreement with experimental results. Independent of whether the dissociation of $\text{H}_2\text{Fe}(\text{CO})_4$ should be referenced to the triplet ground state or first excited singlet state of $\text{Fe}(\text{CO})_4$, the BP86 functional gives good agreement with experimental data for the enthalpy for dissociation of H_2 from $\text{H}_2\text{Fe}(\text{CO})_4$. If, as is currently thought, the reference state for dissociation of $\text{H}_2\text{Fe}(\text{CO})_4$ is the triplet state of $\text{Fe}(\text{CO})_4$, then calculations with the B3LYP functional lead to a value for the bond dissociation enthalpy that is too small. However, if the dissociation process actually should be referenced to the singlet state of $\text{Fe}(\text{CO})_4$, then calculations using the B3LYP functional agree best with experimental data. For either case the BLYP functional does not give good agreement with experimental data for the bond dissociation enthalpy of $\text{H}_2\text{Fe}(\text{CO})_4$.

The oxidative addition of H_2 to $\text{Fe}(\text{CO})_4$, to form $\text{H}_2\text{Fe}(\text{CO})_4$, involves $(\eta^2\text{-H}_2)\text{Fe}(\text{CO})_4$ as an intermediate which has a low activation barrier for breaking the H–H bond. The reaction is expected to involve a curve crossing from a triplet to a singlet potential energy surface.

Acknowledgment. We acknowledge support of this work by the National Science Foundation under Grant CHE90-24509. We also acknowledge a grant of computer time from the San Diego Supercomputer Center which allowed us to perform the

DFT calculations. We also acknowledge informative discussions with Professors George Schatz and Don Ellis.

References and Notes

- (1) Veillard, A. *Chem. Rev.* **1991**, *91*, 743.
- (2) Salahub, D. R.; Zerner, M. C., Eds. *The Challenge of d and f Electrons. Theory and Computation*; ACS Symposium Series 394; American Chemical Society: Washington, DC, 1989.
- (3) Lüthi, H. P.; Siegbahn, P. E. M.; Almlöf, J. *J. Phys. Chem.* **1985**, *89*, 2156.
- (4) Barnes, L. A.; Rosi, M.; Bauschlicher, C. W. *J. Chem. Phys.* **1991**, *94*, 2031.
- (5) (a) Ehlers, A. W.; Frenking, G. *J. Am. Chem. Soc.* **1994**, *116*, 1514. (b) Ehlers, A. W.; Frenking, G. *Organometallics* **1995**, *14*, 423. (c) Dapprich, S.; Frenking, G. *Angew. Chem., Int. Ed. Engl.* **1995**, *34*, 354. (d) Ehlers, A. W.; Dapprich, S.; Vyboishchikov, S. F.; Frenking, G. *Organometallics* **1996**, *15*, 105.
- (6) Blomberg, M. R. A.; Siegbahn, P. E. M.; Lee, T. J.; Rendell, A. P.; Rice, J. E. *J. Chem. Phys.* **1991**, *95*, 5898.
- (7) Barnes, L. A.; Liu, B.; Lindh, R. *J. Chem. Phys.* **1993**, *98*, 3978.
- (8) Persson, B. J.; Roos, B. O.; Pierloot, K. *J. Chem. Phys.* **1994**, *101*, 6810.
- (9) Hohenberg, P.; Kohn, W. *Phys. Rev. B* **1964**, *136*, 864.
- (10) Kohn, W.; Sham, L. J. *Phys. Rev. A* **1965**, *140*, 1133.
- (11) Parr, R. G.; Yang, W. *Density Functional Theory of Atoms and Molecules*; Oxford University: New York, 1988.
- (12) (a) Ziegler, T. *Chem. Rev.* **1991**, *91*, 651. (b) Ziegler, T.; Tschinke, V. In *Density Functional Methods in Chemistry*; Labanowski, J. K., Andzelm, J. W., Eds.; Springer-Verlag: New York, 1991. (c) Fan, L.; Ziegler, T. In *Density Functional Theory of Molecules, Clusters, and Solids*; Ellis, D. E., Ed.; Kluwer Academic: Dordrecht, The Netherlands, 1995.
- (13) Li, J.; Schreckenbach, G.; Ziegler, T. *J. Am. Chem. Soc.* **1995**, *117*, 486.
- (14) Jonas, V.; Thiel, W. *J. Chem. Phys.* **1995**, *102*, 8474.
- (15) Delley, B.; Wrinn, M.; Lüthi, H. P. *J. Chem. Phys.* **1994**, *100*, 5785.
- (16) (a) Ricca, A.; Bauschlicher, C. W. *J. Phys. Chem.* **1994**, *98*, 12899. (b) Ricca, A.; Bauschlicher, C. W. *J. Phys. Chem.* **1995**, *99*, 5922.
- (17) Furet, E.; Weber, J. *Theor. Chim. Acta* **1995**, *91*, 157.
- (18) Eriksson, L. A.; Pettersson, L. G. M.; Siegbahn, P. E. M.; Wahlgren, U. *J. Chem. Phys.* **1995**, *102*, 872.
- (19) Ricca, A.; Bauschlicher, C. W. *Theor. Chim. Acta* **1995**, *92*, 123.
- (20) (a) Collman, J. P.; Hegedus, L. S.; Norton, J. R.; Finke, R. G. *Principles and Applications of Organotransition Metal Chemistry*; University Science Books: Mill Valley, CA, 1987. (b) Crabtree, R. H. *The Organometallic Chemistry of the Transition Metals*; Wiley: New York, 1994. (c) Parshall, G. W.; Ittel, S. D. *Homogeneous Catalysis*; Wiley: New York, 1992.
- (21) See, e.g.: (a) Saillard, T.-Y.; Hoffmann, R. *J. Am. Chem. Soc.* **1984**, *106*, 2006. (b) Hay, P. J. *J. Am. Chem. Soc.* **1987**, *109*, 705. (c) Jean, Y.; Eisenstein, O.; Volatron, F.; Maoche, B.; Sefta, F. *J. Am. Chem. Soc.* **1986**, *108*, 6587. (d) Sargent, A. L.; Hall, M. B.; Guest, M. F. *J. Am. Chem. Soc.* **1992**, *114*, 517. (e) Musaev, D. G.; Morokuma, K. *J. Am. Chem. Soc.* **1995**, *117*, 799. (f) Abu-Hasanayn, F.; Goldman, A. S.; Krogh-Jespersen, K. *J. Phys. Chem.* **1993**, *97*, 5890.
- (22) Wang, W.; Narducci, A.; House, P.; Weitz, E. *J. Am. Chem. Soc.* **1996**, *118*, 8654.
- (23) For a recent review, see: Poliakoff, M.; Weitz, E. *Acc. Chem. Res.* **1987**, *20*, 408.
- (24) McNeill, E. A.; Scholer, F. R. *J. Am. Chem. Soc.* **1977**, *99*, 6243.
- (25) Hay, P. J.; Wadt, W. R. *J. Chem. Phys.* **1985**, *82*, 299.
- (26) (a) Ditchfield, R.; Hehre, W. J.; Pople, J. A. *J. Chem. Phys.* **1971**, *54*, 724. (b) Hehre, W. J.; Ditchfield, R.; Pople, J. A. *J. Chem. Phys.* **1972**, *56*, 2257.
- (27) Wachters, A. J. H. *J. Chem. Phys.* **1970**, *52*, 1033.
- (28) Hay, P. J. *J. Chem. Phys.* **1977**, *66*, 4377.
- (29) Hariharan, P. C.; Pople, J. A. *Chem. Phys. Lett.* **1980**, *66*, 217.
- (30) Rappe, A. K.; Smedley, T. A.; Goddard, W. A. *J. Phys. Chem.* **1981**, *85*, 2607.
- (31) Ehlers, A. W.; Böhme, M.; Dapprich, S.; Gobbi, A.; Höllwarth, A.; Jonas, V.; Köhler, K. F.; Stegmann, R.; Veldkamp, A.; Frenking, G. *Chem. Phys. Lett.* **1993**, *208*, 111.
- (32) Dunning, T. H. *J. Chem. Phys.* **1971**, *55*, 716.
- (33) Becke, A. D. *Phys. Rev. A* **1988**, *38*, 3098.
- (34) Perdew, J. P. *Phys. Rev. B* **1986**, *33*, 8822.
- (35) (a) Lee, C.; Yang, W.; Parr, R. G. *Phys. Rev. B* **1988**, *37*, 785. (b) Miehlich, B.; Savin, A.; Stoll, H.; Preuss, H. *Chem. Phys. Lett.* **1989**, *157*, 200.
- (36) Becke, A. D. *J. Chem. Phys.* **1993**, *98*, 5648.
- (37) Vosko, S. H.; Wilk, L.; Nusair, M. *Can. J. Phys.* **1980**, *58*, 1200.
- (38) (a) Roothaan, C. C. J. *Rev. Mod. Phys.* **1951**, *23*, 69. (b) Pople, J. A.; Nesbet, R. K. *J. Chem. Phys.* **1954**, *22*, 571.
- (39) Pople, J. A.; Gill, P. M. W.; Johnson, B. G. *Chem. Phys. Lett.* **1992**, *199*, 557.
- (40) Schlegel, H. B. *J. Comput. Chem.* **1982**, *3*, 214.
- (41) Pople, J. A.; Krishnan, R.; Schlegel, H. B.; Binkley, J. S. *Int. J. Quantum Chem. Symp.* **1979**, *13*, 225.
- (42) Gaussian 94, Rev. B.1: Frisch, M. J.; Trucks, G. W.; Schlegel, H. B.; Gill, P. M. W.; Johnson, B. G.; Robb, M. A.; Cheeseman, J. R.; Keith, T.; Petersson, G. A.; Montgomery, J. A.; Raghavachari, K.; Al-Laham, M. A.; Zakrzewski, V. G.; Ortiz, J. V.; Foresman, J. B.; Cioslowski, J.; Stefanov, B. B.; Nanayakkara, A.; Challacombe, M.; Peng, C. Y.; Ayala, P. Y.; Chen, W.; Wong, M. W.; Andres, J. L.; Replogle, E. S.; Gomperts, R.; Martin, R. L.; Fox, D. J.; Binkley, J. S.; Defrees, D. J.; Baker, J.; Stewart, J. J. P.; Head-Gordon, M.; Gonzalez, C.; Pople, J. A. Gaussian, Inc., Pittsburgh, PA, 1995.
- (43) Gaussian 92, Rev. E.1: Frisch, M. J.; Trucks, G. W.; Head-Gordon, M.; Gill, P. M. W.; Wong, M. W.; Foresman, J. B.; Johnson, B. G.; Schlegel, H. B.; Robb, M. A.; Replogle, E. S.; Gomperts, R.; Andres, J. L.; Raghavachari, K.; Binkley, J. S.; Gonzalez, C.; Martin, R. L.; Fox, D. J.; Defrees, D. J.; Baker, J.; Stewart, J. J. P.; Pople, J. A. Gaussian, Inc., Pittsburgh, PA, 1992.
- (44) (a) Beagley, B.; Schmidling, D. G. *J. Mol. Struct.* **1974**, *22*, 466. (b) Braga, D.; Grepioni, F.; Orpen, A. G. *Organometallics* **1993**, *12*, 1481.
- (45) Poliakoff, M.; Turner, J. J. *J. Chem. Soc., Dalton Trans.* **1974**, 2276.
- (46) Barton, T. J.; Grinter, R.; Thomson, A. J.; Davies, B.; Poliakoff, M. *J. Chem. Soc., Chem. Commun.* **1977**, 841.
- (47) (a) Seder, T. A.; Ouder Kirk, A. J.; Weitz, E. *J. Chem. Phys.* **1986**, *85*, 1977. (b) Weitz, E. *J. Phys. Chem.* **1994**, *98*, 11256.
- (48) (a) Adamo, C.; Lelj, F. *J. Chem. Phys.* **1995**, *103*, 10605. (b) Castro, M.; Salahub, D. R.; Fournier, R. *J. Chem. Phys.* **1994**, *100*, 8233.
- (49) Villalta, P. W.; Leopold, D. G. *J. Chem. Phys.* **1993**, *98*, 7730.
- (50) (a) Ryther, R. J.; Weitz, E. *J. Phys. Chem.* **1991**, *95*, 9841. (b) Ryther, R. J.; Weitz, E. *J. Phys. Chem.* **1992**, *96*, 2561.
- (51) Lewis, K. E.; Golden, D. M.; Smith, G. P. *J. Am. Chem. Soc.* **1984**, *106*, 3905.
- (52) (a) Farmery, K.; Kilner, M. *J. Chem. Soc. A* **1970**, 634. (b) Stobart, S. R. *J. Chem. Soc., Dalton Trans.* **1972**, 2442. (c) Bradley, G. F.; Stobart, S. R. *J. Chem. Soc., Chem. Commun.* **1975**, 325.
- (53) (a) Eyermann, C. J.; Chung-Phillips, A. *J. Am. Chem. Soc.* **1984**, *106*, 7437. (b) Dedieu, A.; Nakamura, S. *J. Organomet. Chem.* **1984**, *260*, C63. (c) Pensak, D. A.; McKinney, R. J. *Inorg. Chem.* **1979**, *18*, 3407.
- (54) Dedieu, A.; Nakamura, S.; Sheldon, J. C. *Chem. Phys. Lett.* **1987**, *141*, 323.
- (55) Bauschlicher, C. W. *Chem. Phys. Lett.* **1995**, *246*, 40.
- (56) For recent reviews of dihydrogen species, see: (a) Kubas, G. J. *Acc. Chem. Res.* **1988**, *21*, 120. (b) Crabtree, R. H. *Acc. Chem. Res.* **1990**, *23*, 95. (c) Heinekey, D. M.; Oldham, W. J., Jr. *Chem. Rev.* **1993**, *93*, 913.
- (57) Ziegler, T.; Tschinke, V.; Fan, L.; Becke, A. D. *J. Am. Chem. Soc.* **1989**, *111*, 9177.